Applied Catalysis B: Environmental 90 (2009) 535–544

Contents lists available at ScienceDirect

Applied Catalysis B: Environmental

journal homepage: www.elsevier.com/locate/apcatb

Ceria–zirconia-supported rhodium catalyst for NO_x reduction from coal combustion flue gases

Małgorzata Adamowska [a,b,d], Andrzej Krztoń [a], Mieczysława Najbar [c], Józef Camra [c], Gérald Djéga-Mariadassou [d], Patrick Da Costa [d,*]

[a] Centre of Polymer and Carbon Materials, Polish Academy of Sciences, M. Curie-Skłodowskiej 34, 41-819 Zabrze, Poland
[b] Silesian University of Technology, Faculty of Chemistry, Strzody 9, 44-100 Gliwice, Poland
[c] Jagiellonian University, Faculty of Chemistry, Ingardena 3, 30-060 Kraków, Poland
[d] UPMC Paris 6, Laboratoire de Réactivité de Surface, CNRS, UMR 7197, 4 place Jussieu, 75252 Paris Cedex 05, France

ARTICLE INFO

Article history:
Received 5 March 2009
Received in revised form 7 April 2009
Accepted 9 April 2009
Available online 19 April 2009

Keywords:
Lean deNO$_x$ of coal
Ceria–zirconia
Rhodium
Mechanism

ABSTRACT

The catalytic activities of ceria–zirconia mixed oxides $Ce_xZr_{1-x}O_2$ ($x = 0.17$, 0.62 and 0.8) rhodium catalysts were determined by isothermal steady-state experiments using a representative mixture of exhaust gases of coal combustion. Results show that all supports are active in deNO$_x$ reaction in the presence of the mentioned gas mixture. However, their catalytic activity varies with the content of cerium and goes through a maximum for $x = 0.62$, leading to 27% NO_x consumption. The effect of rhodium on $Ce_{0.62}Zr_{0.38}O_2$ considerably improves the catalytic activity during the deNO$_x$ process assisted by hydrocarbons. The rhodium addition decreases by about 34 °C the temperature of NO_x consumption, which goes up to 57%. A mechanism of hydrocarbon (HC) assisted reduction of NO is proposed on ceria–zirconia-supported rhodium catalysts. This mechanism is divided in three catalytic cycles involving (i) the oxidation of NO into NO_2, (ii) the reaction of NO_2 and the hydrocarbons leading to RNO_x species and $C_xH_yO_z$, and finally (iii) the decomposition of NO assisted by these latter $C_xH_yO_z$ species.

1. Introduction

Removal of nitrogen oxides present in flue gases from fossil fuel combustions is one of the targets of environmental catalysis. Selective catalytic reduction by ammonia (NH_3–SCR) is the main industrial catalytic technology for abatement of nitrogen oxides emission from coal combustion. However, requirement for large-scale NH_3–SCR reactors linked to high storage of ammonia, can lead to environmental contamination. As a consequence this process in urban site and for small or medium scale boilers should be avoided [1]. Selective catalytic reduction by hydrocarbons (HC–SCR), and more particularly by methane is a process quite more attractive for NO_x abatement from flue gases produced by natural gas combustion; this process has not yet reached industrial application. Similarly SCR of NO_x by aliphatic and aromatic hydrocarbons, the key pollutants contained in gases evolved from coal combustion, seems to be interesting for coal boilers.

A large number of catalysts have been evaluated in the selective catalytic reduction (SCR) of NO_x by hydrocarbons [1,2]. These catalysts are mainly metal ion-exchanged zeolites (e.g. Cu, Co, Fe and Pt) and supported platinum group metals (PGMs) such as Pt, Pd, Rh and Ag, on various metal oxides (e.g. Al_2O_3, TiO_2 and CeO_2) [1–5]. However, the rather poor stability of metal ion-exchanged zeolites and the deactivation of base metal oxides in the presence of water in the feed constitute the main drawbacks of these catalysts to be used under real lean conditions [1]. Moreover, supported PGMs exhibit rather low selectivity to N_2, N_2O being formed in substantial amounts [2]. These latter catalysts have mostly been supported on SiO_2 or Al_2O_3 [2] and very little attention has been paid to other supports such as ceria–zirconia.

However, it is well known that these oxides (ceria and Ce-containing mixed oxides) have attracted much attention because of their high oxygen storage capacity (OSC) and unique redox properties. CeO_2 is able to undergo rapid reduction/oxidation cycles according to the reaction $2CeO_2 \Leftrightarrow Ce_2O_3 + (1/2)O_2$. However, pure CeO_2 is not used a support due to its poor thermal stability. The addition of ZrO_2 to ceria strongly improves ceria oxygen storage capacity, redox property, thermal resistance and better catalytic activity at lower temperatures [6–8].

Thus, only few studies have deal for ceria–zirconia-based catalysts for the SCR of NO_x by propene. (i) Orlik et al. [9] on Rh/$CeZrO_2$, (ii) Centi et al. [10] on Pt/$Ce_{0.50}Zr_{0.50}O_2$/Al_2O_3 and (iii) Liotta et al. [11] on Pt/$Ce_{0.50}Zr_{0.50}O_2$. More recently, Thomas et al.

* Corresponding author at: UPMC Paris 6, Laboratoire de Réactivité de Surface, CNRS, UMR 7197, Case 178, 4 place Jussieu, 75252 Paris Cedex 05, France.
Tel.: +33 1 44 27 55 12; fax: +33 1 44 27 60 33.
E-mail address: patrick.da_costa@upmc.fr (P. Da Costa).

0926-3373/$ – see front matter © 2009 Elsevier B.V. All rights reserved.
doi:10.1016/j.apcatb.2009.04.018

have reported on the performances of $Pd/Ce_{0.68}Zr_{0.32}O_2$ (Pd/CZ) catalysts in the SCR of NO_x assisted by C_3H_6 [12]. These catalysts exhibited much higher selectivity to N_2 than Pd^0/SiO_2. This difference was assigned to the occurrence of a $deNO_x$ mechanism on Pd/CZ different from that of the dissociation of NO on zero-valent PGMs atoms [13]. Thomas et al. have also studied the influence of the nature of the noble metal on ceria–zirconia (CZ) catalysts [14]. The authors have shown that the order of reactivity of the PGMs supported on CZ was: Pd > Pt > Rh [14].

The authors have also proposed a deNOx mechanism based on three catalytic cycles. The proposed mechanism was consistent with previous studies of Djéga-Mariadassou and Boudart [15,16] and Ferreira et al. [17]. In this model, CZ achieved both NO oxidation to NO_2 (cycle 1) and NO decomposition to N_2 (cycle 3), whereas PdO_x activated propylene via ad-NO_2 species (cycle 2) producing R-NO_x compounds that then decomposed to NO and $C_xH_yO_z$ [18]. The role of the intermediate oxygenates is to reduce CZ to provide the catalytic sites responsible for NO decomposition [12,14,15,17].

In the literature, the reductants involved in HC–SCR processes are mainly simulated with light aliphatics and only few studies are reported with aromatic hydrocarbons as reductants [3,7]. However, both aliphatic and aromatic hydrocarbons (HC) are the major pollutants of gases from coal combustion; they can be simultaneously eliminated within the $deNO_x$ process [8]. More recently, we have shown that CZ are active for HC–SCR with a series of reducing agents representative of flue gases from coal combustion [19,20].

The aim of this work is to investigate the influence of rhodium addition to a ceria–zirconia support on lean $deNO_x$ reaction with a series of reducing agents such as aromatics (e.g. benzene, toluene and xylene) or aliphatic hydrocarbons (e.g. propane and propene), representative of exhaust gases from small and medium scale boilers [8]. To our knowledge, such catalysts have not been investigated for coal $deNO_x$ reaction. We first present the influence of catalyst preparation. Then, based on transient and steady-state experiments, a mechanism of the lean $deNO_x$ is proposed for the CZ-supported rhodium-based catalysts for the flue gas from coal combustion process.

2. Experimental

2.1. Catalyst preparation

2.1.1. Ceria–zirconia ($Ce_xZr_{1-x}O_2$, CZ)

The CZ solid solutions were provided by Rhodia. The samples were reduced under pure H_2 (air liquide) for 2 h at 500 °C with a flow rate of 40 $mL_{NTP}\,min^{-1}$ of H_2 per gram of catalyst and finally gently exposed to air at RT. Such a preparation was performed for the sake of comparison with noble metal catalyst synthesis.

2.1.2. Rh_{Cl}/CZ

The CZ-supported rhodium ex-chloride catalyst (0.31 wt% Rh) was prepared by anionic exchange from an acidic solution of rhodium chloride ($RhCl_3, 3H_2O$, Johnson Matthey) with the support [21]. The acidic solution of rhodium chloride was added to an aqueous suspension of CZ (pH 1.9). This suspension was prepared as follows: a hydrochloric acid solution (pH 1.9) prepared by adding HCl to distilled water was added to CZ. Then, the mixture was placed under vigorous stirring for 2 h. After being exchanged, Rh(0.40)/CZ was filtered and washed with distilled water before being dried in air at 120 °C for 3 h. This sample was then reduced under pure H_2 (air liquide) for 1 h at 500 °C with a flow rate of 40 $mL_{NTP}\,min^{-1}$ of H_2 per gram of catalyst and finally gently exposed to air at RT.

2.1.3. Rh_N/CZ

The CZ-supported rhodium ex-nitrate catalyst (0.52 wt% Rh) was prepared by incipient wetness impregnation from aqueous solutions of Rh(III) nitrate (Johnson Matthey) [22]. After impregnation, Rh_N/CZ was dried in air at 110 °C for 24 h. This sample was then reduced under pure H_2 (air liquide) for 1 h at 300 °C with a flow rate of 40 $mL_{NTP}\,min^{-1}$ of H_2 per gram of catalyst and finally gently exposed to air at RT.

2.2. Catalyst characterization

Metal and chlorine contents were determined by chemical analyses (CNRS—Vernaison) or by EDS. Chlorine contents were about 1.6 wt% for CZ-supported catalyst. The specific surface areas were determined by physisorption of N_2 at 77 K using a Quantasorb Jr. dynamic system equipped with a thermal conductivity detector (TCD). The specific surface areas were calculated using the BET method.

2.2.1. Determination of the percentage of exposed zero-valent metal atom (PME^0)

With the well-known reducibility of the CZ support [23], the determination of the percentage of exposed zero-valent metal atom was done by means of benzene hydrogenation [24]. Briefly, prior to benzene hydrogenation, the catalyst sample (50 mg deposited on sintered glass of a pyrex reactor) was heated in flowing H_2 (100 $mL_{NTP}\,min^{-1}$) at atmospheric pressure with a heating rate of 3 °C min^{-1} up to 300 °C and was kept at this temperature for 2 h. After cooling to 50 °C under H_2, the reaction was started. For a sake of comparison, one catalyst was treated in H_2, then treated in O_2 (5%)/Ar at same temperature prior benzene hydrogenation. The partial pressure of benzene was 51.8 Torr, and the total flow rate was 107 $mL_{NTP}\,min^{-1}$ with H_2 as balance. The composition of the effluents was analyzed by means of online gas chromatographs (Hewlett–Packard 5890, FID) equipped with a capillary column (PONA, HP, 50 m long, 0.20 mm inner diameter, 0.5 μm film thickness). The only detected product was cyclohexane. From the initial reaction rates, the numbers of exposed zero-valent metal atoms were calculated according to turnover rate of 0.22 s^{-1} for benzene hydrogenation reaction carried out at 50 °C.

2.2.2. Determination of the state of rhodium

X-ray photoelectron spectroscopy was used to determine the chemical composition of the surface nanolayers of the freshly prepared catalyst as well as of the thermally treated catalysts. The measurements were conducted using an ESCA 150 Vacuum Science Workshop with an aluminium anode as an X-ray source, resulting in a surface sensitivity of approximately 2 nm [25].

2.2.3. Determination and identification of rhodium particles on CZ

TEM specimens were prepared by crushing the catalyst on ethanol and dispersing the catalyst onto holey-carbon covered TEM grid. HRTEM was performed on a JEOL 2010 UHR electron microscope operating at 200 keV, with a nominal point to point resolution of 1.9 Å. Image analysis was performed using ADOBE Photoshop software. Rhodium oxide phase was identified by Fourier analysis of HRTEM images, which provide precise measurements of their lattice spacings and interplanar angles. Because each rhodium oxide phase exhibits characteristic lattice spacings and interplanar angles that are unique to each phase, this procedure enables their identification. During the same analyses, emission dispersive spectroscopy (EDS) measurements were performed to verify the presence of rhodium using the same microscope.

2.3. Catalytic runs

These experiments were carried out in a U-type quartz reactor (20 mm inner diameter). The sample (0.8 g) was held between plugs of quartz wool and the temperature was controlled through a Eurotherm 7840 temperature controller using a K-type thermocouple. Reactant gases were fed from independent mass flow controllers (Brooks 5850E). The total flow was 250 $mL_{NTP}\,min^{-1}$ to which corresponds a hour space velocity (GHSV) of 30,000 h^{-1}.

Prior to catalytic runs, the samples were calcined in situ in dry air at 500 °C (heating rate up to 500 °C was 10 °C min^{-1}) for 2 h with a flow rate of 500 $mL_{NTP}\,min^{-1}\,g^{-1}$. Steady-state and temperature-programmed desorption (TPD) experiments were carried out. After being contacted with the appropriate gas mixture at RT, TPD experiments were carried out from RT to 500 °C with a heating rate of 3 °C min^{-1}. Before TPD experiments, the catalyst samples were flushed in N_2 to remove physisorbed species from the adsorption mixture.

Temperature-programmed surface reaction (TPSR) were carried out from room temperature (RT) to 500 °C with a heating rate of 3 °C min^{-1} using the following gas mixture: 250 ppm NO, 247 ppm hydrocarbon mixture (50 ppm propane, 133 ppm propene and 64 ppm toluene) and 5% O_2 in Argon. 247 ppm hydrocarbon mixture corresponds to 1000 ppm of C_1.

Isothermal steady-state experiments were performed with the same gas mixture composition from 170 to 500 °C with the same heating rate. The reactor outflow was analyzed using the combination of four different detectors.

An Eco Physics CLD 700 AL chemiluminescence NO_x analyzer (for NO and total NO_x) allowed the simultaneous detection of both NO, NO_2 and NO_x. Ultramat 6 IR analyzers were used to the monitoring of N_2O, CO, CO_2 and one FID detector (FIDAMAT 5E) was used to determine the total concentration of hydrocarbons.

3. Results and discussion

3.1. $Ce_xZr_{1-x}O_2$ mixed oxides

The catalytic activity of ceria–zirconia mixed oxides $Ce_xZr_{1-x}O_2$ (x = 0.17, 0.62 and 0.8) was determined by isothermal steady-state experiments for these three formulations in the presence of a (toluene–propane–propene) mixture (Table 1). The highest conversion of NO_x to N_2 (27% at 322 °C, in Table 1) was achieved for $Ce_{0.62}Zr_{0.38}O_2$ a commercial catalyst of Rhodia. The other supports $Ce_{0.8}Zr_{0.2}O_2$ and $Ce_{0.17}Zr_{0.83}O_2$ have shown lower conversions (22 and 19%, respectively). Our results confirm those obtained by Terribile et al. [26] in which the most active $Ce_xZr_{1-x}O_2$ were those with x ranging from 0.6 to 0.8. Then, the support $Ce_{0.62}Zr_{0.38}O_2$ was selected to be impregnated by the rhodium for deNO_x studies.

Table 1
Steady-state NO_x reduction activity of supports $Ce_xZr_{1-x}O_2$, using toluene–propane–propene as reductants (247 ppm), NO (250 ppm) and O_2 (5%).

Catalysts	Maximum of NO_x conversion	
	T (°C)	%
$Ce_{0.8}Zr_{0.2}O_2$	312	22
$Ce_{0.63}Zr_{0.37}O_2$	322	27
$Ce_{0.16}Zr_{0.84}O_2$	324	19

Table 2
Surface area (BET) and percentage of exposed metal measured by Benzene hydrogenation after reduction at 300 °C in hydrogen.

Catalysts	S_{BET} ($m^2\,g^{-1}$)	Rh^0
Rh_N/CZ	88	50
Rh_{Cl}/CZ	85	23

3.2. $Rh/Ce_{0.62}Zr_{0.38}O_2$ catalysts

Table 2 lists the surface area measurement and the percentage of exposed Rh^0 of ceria–zirconia-supported catalysts of the rhodium-based catalysts. The surface area is 88 and 85 $m^2\,g^{-1}$ for Rh_N/CZ and Rh_{Cl}/CZ, respectively, whereas 105 $m^2\,g^{-1}$ are found on CZ before and after testing. The percentage of exposed zero-valent Rh atoms is 50 and 23% for Rh_N/CZ and Rh_{Cl}/CZ, respectively. When catalyst is reduced in H_2 up to 300 °C, then treated in Ar/(5% O_2) at the same temperature, the percentage of exposed zero-valent Rh atoms is then 0%. From these results, we can conclude that the rhodium should be in an oxidation state different than zero in lean deNO_x conditions.

3.2.1. State of rhodium on CZ

The oxidation states of rhodium were provided by XPS analyses. The results are presented in Fig. 1. Rh 3d XP-spectra of a ceria–zirconia-supported Rh catalyst are shown after runs in reaction mixture (NO, O_2, Ar and hydrocarbon mixture) for 1 h at temperature 500 °C followed by a cooling in argon up to RT. The Rh_N/CZ (Fig. 1(a)) and Rh_{Cl}/CZ (Fig. 1(b)) measured spectra were peak-fitted with three components, one for metallic Rh and two for Rh^{3+} (Rh_2O_3). Furthermore, more than 80% of rhodium is in 3+ oxidation state.

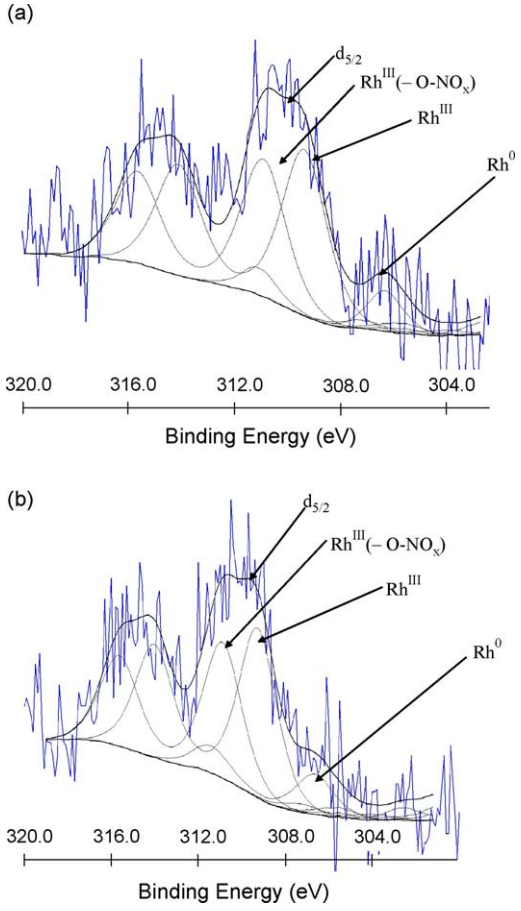

Fig. 1. Rh 3d photoelectron spectra of Rh supported on ceria–zirconia after runs in reaction mixture (247 ppm hydrocarbon mixture (propane, propene and toluene), 250 ppm NO, 5% O_2, GHSV = 30,000 h^{-1}) (a) $Rh/Ce_{0.625}Zr_{0.375}O_2$ (nitrate precursor) and (b) $Rh/Ce_{0.625}Zr_{0.375}O_2$ (chloride precursor).

Table 3
X-ray photoelectron spectroscopy of Rh($3d_{5/2}$) binding energy for ceria–zirconia-supported rhodium catalysts.

	Rh^{3+} (ONO)	Rh^{3+}	Rh^0
Rh_N/CZ	310.4	309.2	306.3
Rh_{Cl}/CZ	310.9	309.3	306.7

Table 3 presents the results obtained on Rh-based catalysts. The Rh $3d_{5/2}$ peak positions in the range of 306.3–306.7 eV can be assigned to Rh^0 [25]. It was well known, that irreducible Rh oxide phase can be characterised by its high binding energy of the Rh 3d photoelectron peak (309.3–309.9 eV) in comparison with that of Rh^{3+} (308.1–308.6 eV) [27,28]. The Rh $3d_{5/2}$ peak positions in the range of 309.3–309.9 eV can be assigned to RhO_2 (i.e. Rh^{4+}), but also non-stoichiometric Rh_2O_3, where O/Rh ratio is in excess of 1.5 in the outermost layers of Rh_2O_3, is suggested as an explanation for the unusually high binding energy values [29,30]. Finally, for Rh_N/

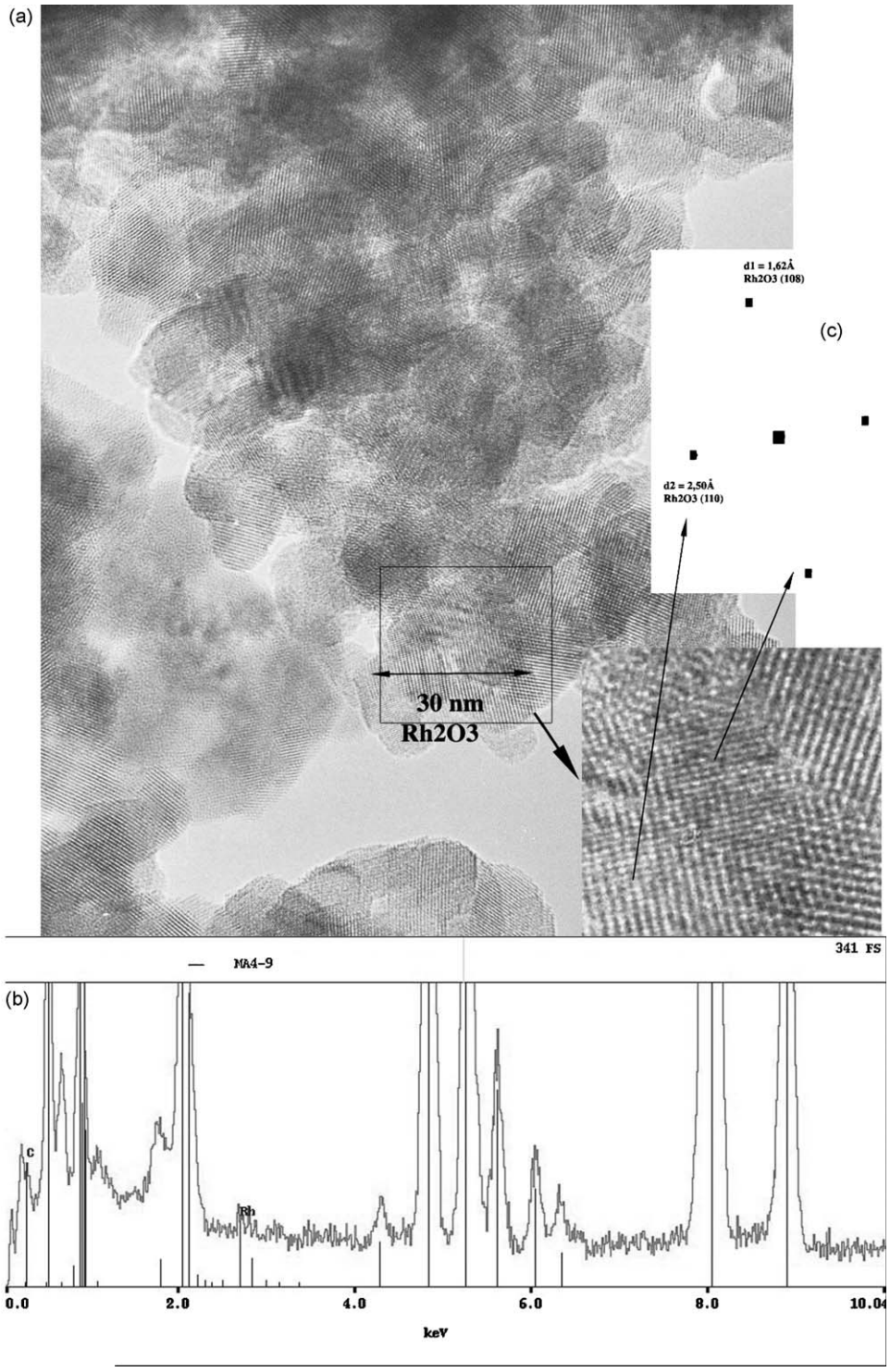

Fig. 2. Transition electron microscopy of Rh supported on ceria–zirconia catalyst Rh_N/CZ, coupled with EDS spectroscopy and diffraction.

CZ and Rh_{Cl}/CZ catalysts (Table 3), the Rh $3d_{5/2}$ peak positions in the range of 309.2 and 309.3 eV is assignated to Rh^{3+}. The higher Rh $3d_{5/2}$ peak positions cannot be attributed to Rh^{4+}. However, these positions can be attributed to rhodium in 3+ oxidation state with some nitrite or nitrate ligands forming as result of NO or NO_2 adsorption non-Rh or O ions (BE = 31034 and 310.9 eV, respectively) (Fig. 1 and Table 3).

3.2.2. Rh_2O_3 particles on CZ

From percentage of metal exposed (PME), one can conclude that rhodium should be present in an oxidation state different than zero. Rhodium could then be present in a cationic form surrounded by oxygen atoms or in RhO or Rh_2O_3 phases.

From TEM and EDS analyses, one can conclude that rhodium is well dispersed on the CZ support since rhodium was detected for each analyzed zone. In Fig. 2(a) is reported a TEM image from Rh_N/CZ catalyst. EDS led to the conclusion that rhodium is present on the analyzed zone (Fig. 2(b)). From this image, HRTEM was performed. Rhomboedric particles of Rh_2O_3 were then detected. The diffractogram of the particle (Fig. 2(c)) reveals the (1 1 0) reflection occurring form the rhomboedric Rh_2O_3 phase. The analyzed particle is constituted to two or three layers of atoms. This rhomboedric phase was confirmed by Fourier analyses of HRTEM images as already reported [27].

In conclusion, rhodium should be present as well in 3+ oxidation state and in rhomboedric particles of Rh_2O_3.

3.2.3. Catalytic activity of ceria–zirconia-supported rhodium catalysts

TPSR and isothermal steady-state experiments were carried out on $Rh/Ce_{0.62}Zr_{0.38}O_2$ catalysts obtained from rhodium chloride and rhodium nitrate precursors. During the deNO_x process, it is well known that NO oxidation and NO dissociation are essential steps [12,14,15].

3.2.3.1. NO oxidation. The NO oxidation reaction was investigated over CZ and Rh_N/CZ and Rh_{Cl}/CZ under TPSR conditions. As shown in Fig. 3, the NO oxidation is the greatest around 380–400 °C. For higher temperatures, the conversion of NO decreases due to thermodynamic limitations. It is important to note that the addition of Rh promotes significantly the NO oxidation, only in the case of Rh_N/CZ. However, this reaction is also catalyzed by the CZ support, as already shown in the literature [14,18–20]. Thus, the NO oxidation can take place on sites from the support or on sites such as Rh^{3+}.

3.2.3.2. Prediction of NO dissociation temperature. According to Djéga-Mariadassou [15,16], the temperature of NO dissociation can be predicted by NO_x TPD. Hence, the NO_x temperature desorption peaks should correspond to the temperature at which NO_x are converted. Fig. 4 shows the NO_x TPD profiles in Ar/O_2 of samples contacted with $NO–O_2$ (250 ppm, 5%). The NO_x desorption is higher on support alone than on Rh_N/CZ and Rh_{Cl}/CZ. The addition of Rh_N on the support does not affect the TPD profiles to a large extent. In both cases, two NO_x desorption peaks are observed at about 140 and 440 °C. In contrast, the addition of rhodium by chloride precursor leads to a TPD profile different than the support. For Rh_{Cl}/CZ, a board peak which can correspond to the support is observed at about 215 °C and a large peak is centered at 315 °C. Thus, on Rh_{Cl}/CZ catalyst, the NO_x adsorption sites are different than those of the CZ or the Rh_N/CZ catalyst. On CZ-based catalysts, different authors [12,14,15,31–33] have proposed that NO reduction takes place via a lacunar mechanism on reduced CZ sites. They also claimed that N_2 is produced by the decomposition of NO on prereduced cerium oxide surfaces. The same mechanism has also been reported in three-way catalysis using CO as reductant [15,33].

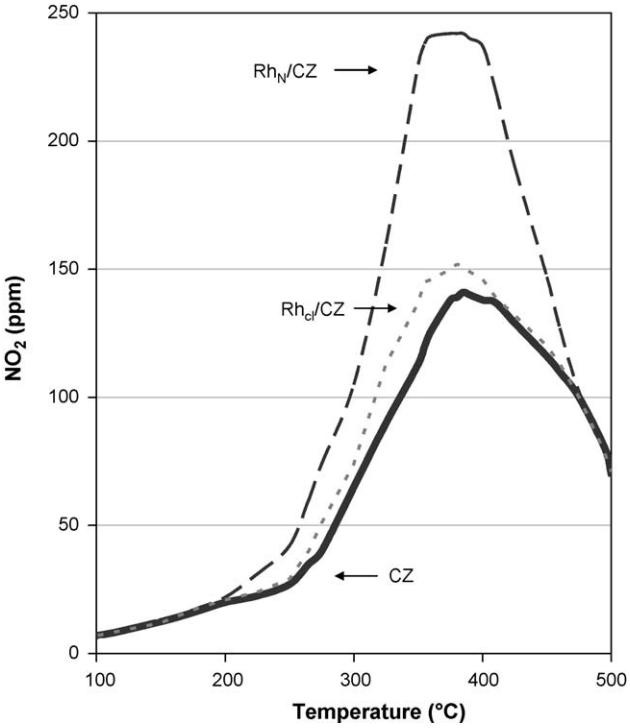

Fig. 3. Evolution of NO_2 concentration in the course of the $NO–O_2$ reaction on CZ support and Rh_{Cl}/CZ and Rh_N/CZ catalyst (250 ppm NO, 5% O_2, balance Ar).

On Rh_N/CZ catalyst, as rhodium is in a high oxidation state, we cannot exclude that rhodium species are not involved in NO decomposition.

The low NO_x desorption of Rh_{Cl}/CZ catalyst can be explained by an inhibition of Cl. According to Force et al. [34], in presence of chlorine, the vacancies that can be present in Rh/CZ catalyst are then occupied. Then, in those conditions, the adsorption of

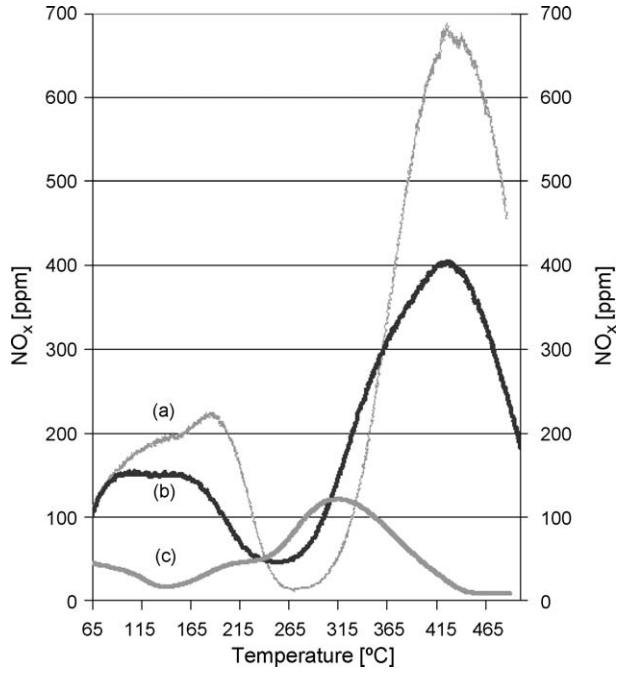

Fig. 4. NO_x temperature-programmed desorption profiles in Ar/O_2 (8%) after exposure of the catalysts to $NO–O_2$ (250 ppm NO, 5% O_2, balance Ar) at RT. (a) $Ce_{0.625}Zr_{0.375}O_2$, (b) $Rh_N/Ce_{0.625}Zr_{0.375}O_2$ (nitrate precursor) and (c) $Rh_{Cl}/Ce_{0.625}Zr_{0.375}O_2$ (chloride precursor).

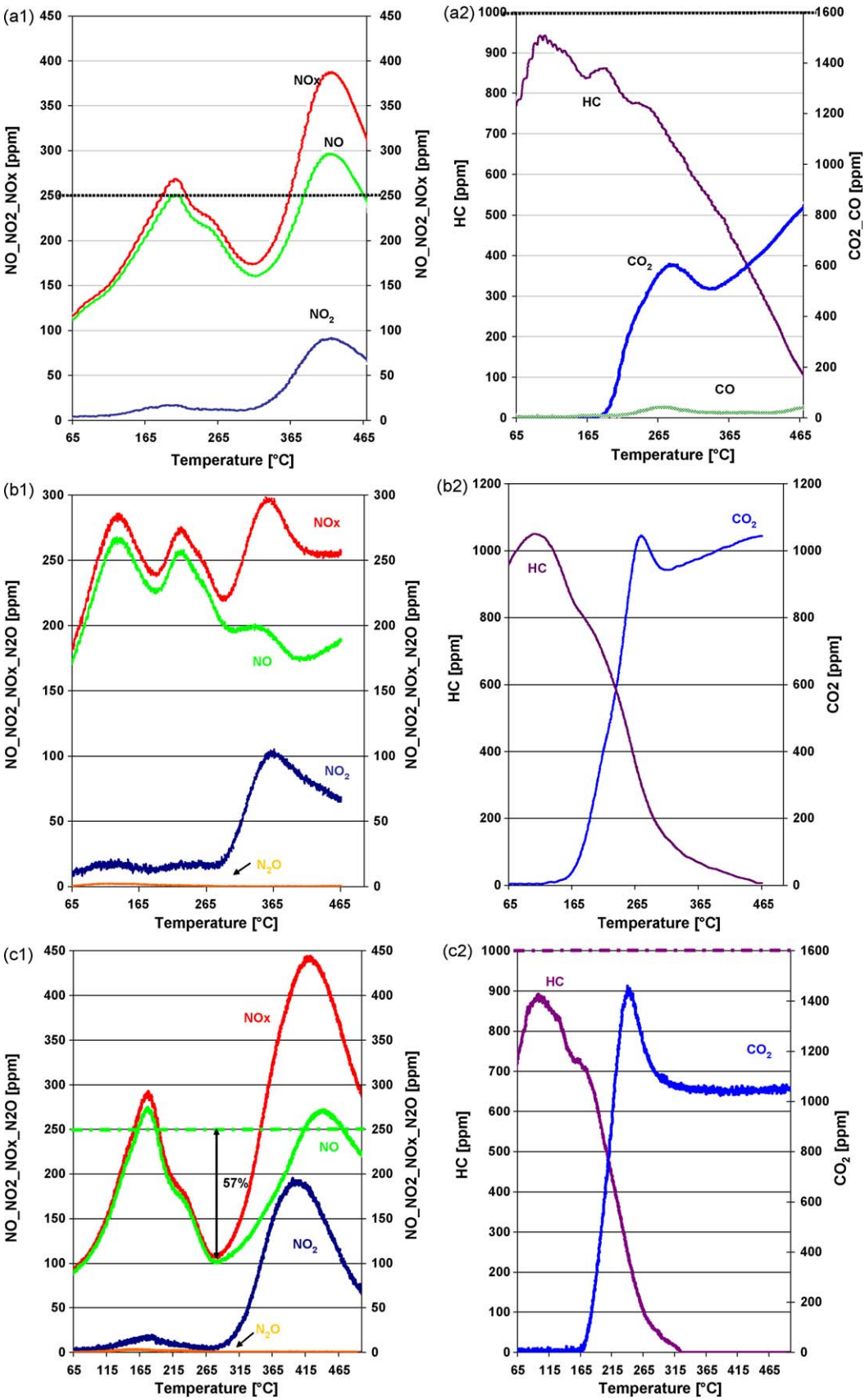

Fig. 5. DeNO$_x$ TPSR profile in the presence of 247 ppm hydrocarbon mixture (propane, propene and toluene), 250 ppm NO, 5% O_2, GHSV = 30,000 h^{-1}; evolution of NO_x, NO, NO_2, N_2O concentrations on (a)-1 $Ce_{0.625}Zr_{0.375}O_2$, (b)-1 $Rh_{Cl}/Ce_{0.625}Zr_{0.375}O_2$, (c)-1 $Rh_N/Ce_{0.625}Zr_{0.375}O_2$; evolution of HC, CO and CO_2 concentrations on (a)-2 $Ce_{0.625}Zr_{0.375}O_2$, (b)-2 $Rh_{Cl}/Ce_{0.625}Zr_{0.375}O_2$ and (c)-2 $Rh_N/Ce_{0.625}Zr_{0.375}O_2$.

molecules such as NO is much more difficult. Consequently, the desorption of NO_x in presence of catalyst containing 1.6 wt% of chlorine is different than that observed on non-containing chlorine one.

3.2.3.3. TPSR of HC–NO–O_2. TPSR of the complete reacting mixture was performed after exposure of CZ, Rh_{Cl}/CZ and Rh_N/CZ catalysts to the reacting mixture at RT (Fig. 5). On CZ and Rh_N/CZ catalysts, the NO desorption is the major NO_x species with a two peak profile (190 and 420 °C) (Fig. 5(a)-1 and (c)-1). The formation of NO_2 only appear at temperatures higher than 250 °C, which is in agreement with the results obtained in NO oxidation (Fig. 3).

On Rh_{Cl}/CZ catalyst, the features are different in terms of NO, with three features observed. However, the NO_2 is only observed at high temperature (Fig. 5(b)-1). On this catalyst, the HC mixture is moderately consumed from 90 to 190 °C, with a HC desorption occurring at about 110 °C and at higher temperatures the oxidation of HC accelerates (Fig. 5(b)-2), then slows down for temperatures higher than 300 °C. The NO_x profile shows a decrease of the NO_x concentration from 265 to 300 °C with a maximum at 275 °C corresponding to 12% of the NO_x inlet concentration. At this temperature, the conversion of HC is 60%. At higher temperatures, the NO_x concentration reaches back its inlet concentration. Furthermore, the NO is oxidised to NO_2 when full conversion of HC is achieved at about 465 °C.

On Rh_N/CZ catalyst (Fig. 5(c)-1 and (c)-2), a large NO_x consumption is observed from 180 to 320 °C, the maximum of conversion is 57% at about 275 °C. At this temperature the HC mixture is highly consumed, with 90% conversion of HC into CO_2. Similar results are found during the TPSR profiles on CZ (Fig. 5(a)-1 and (a)-2). Hence, on support, a maximum of 30% NO_x conversion is found at about 317 °C corresponding to 40% conversion of HC which started to be consumed from 107 °C. However, in comparison to Rh_N/CZ catalyst, the NO_x conversion is shifted to higher temperatures. Indeed, in the presence of rhodium, the temperature of maximum NO_x consumption is decreased by about 34 °C. Thus, the rhodium in high oxidation state (Rh^{3+} and Rh_2O_3), promotes the deNO_x process leading to higher NO_x conversion into N_2 at low temperature.

3.2.3.4. Activity during isothermal steady-state deNO_x reaction. Prior to steady-state measurements, the catalysts were submitted to a TPSR under the complete reacting mixture from RT to 500 °C with a heating rate of 5 °C min^{-1} (Fig. 5). Figs. 6 and 7 show the performances of the catalysts for the reduction of NO_x under isothermal steady-state conditions. The temperature of maximum of N_2 formation, the corresponding NO_x and HC conversions are listed in Table 4.

It is obvious that the introduction of Rh only in nitrate form leads to a significant increase of NO_x reduction to N_2 as well as a large decrease of the HC light-off temperature (Table 4). However, at low temperature (150–250 °C), both CZ and Rh-based catalysts lead to the same activity. From this result, we can propose that the reaction mainly takes place on the bare support. At higher temperature (>250 °C), the activity of Rh_N catalyst is twice than that of the CZ. Then, the active sites are mainly rhodium sites.

Thomas et al. [14] already showed that the addition PGM-based catalysts led to similar results for propene-assisted decomposition of NO on CZ catalysts. Table 4 lists the temperature of light-off of HC over studied catalysts with respect to reaction conditions. Conversion of NO_x to N_2 higher than 50% is obtained on the Rh_N/CZ catalysts. On the other hand, Rh_{Cl}/CZ shows a rather low conversion of NO_x to N_2 (6.4% at 178 °C, in Fig. 6). The obtained conversion is lower than that found for CZ, despite the fact that the light-off temperature of HC is similar to that of the most active CZ-based catalyst (Rh_N/CZ). These differences could be due to the

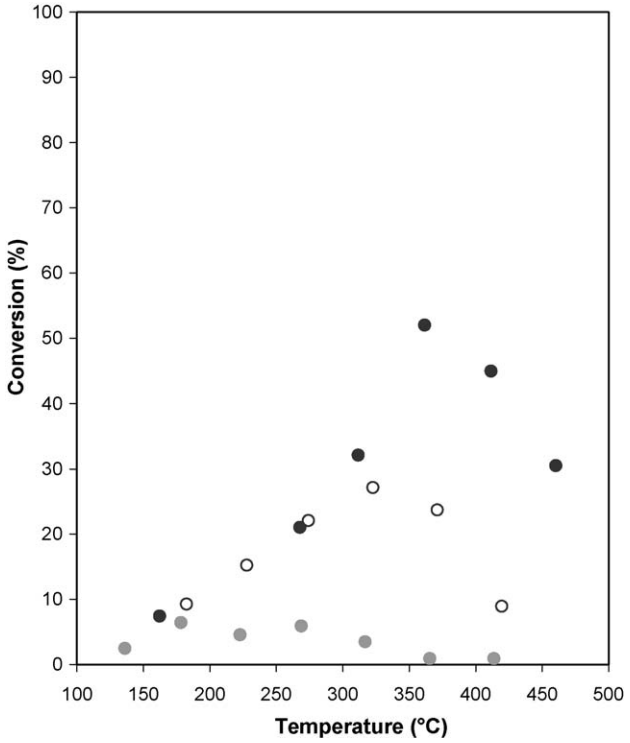

Fig. 6. Evolution of NO_x conversion to N_2 in the course of isothermal steady-state deNO_x reaction on $Ce_{0.625}Zr_{0.375}O_2$ (○), on Rh/$Ce_{0.625}Zr_{0.375}O_2$ (chloride precursor) (●), on Rh/$Ce_{0.625}Zr_{0.375}O_2$ (nitrate precursor) (●), in the presence of 247 ppm hydrocarbon mixture (propane, propene and toluene), 250 ppm NO, 5% O_2, GHSV = 30,000 h^{-1}.

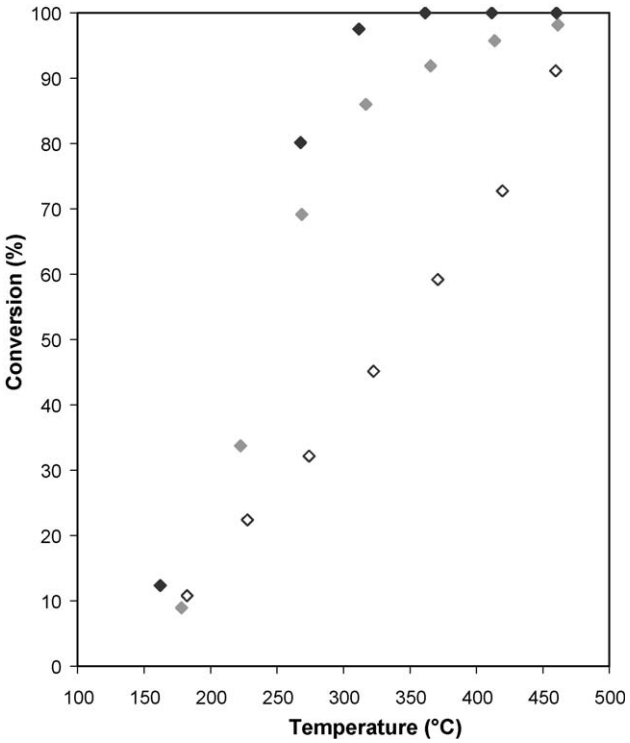

Fig. 7. Evolution of hydrocarbons conversion to CO_2 in the course of isothermal steady-state deNO_x reaction on $Ce_{0.625}Zr_{0.375}O_2$ (◇), on Rh/$Ce_{0.625}Zr_{0.375}O_2$ (chloride precursor) (◆), on Rh/$Ce_{0.625}Zr_{0.375}O_2$ (nitrate precursor) (◆), in the presence of 247 ppm hydrocarbon mixture (propane, propene and toluene), 250 ppm NO, 5% O_2, GHSV = 30,000 h^{-1}.

Table 4
Temperature of maximum of N_2 formation and percentage of NO_x converted to N_2 at this temperature over $Ce_{0.68}Zr_{0.32}O_2$ (CZ) and ceria–zirconia-supported rhodium catalysts (Rh_N/CZ and Rh_{Cl}/CZ) for the steady-state HC–NO–O_2 reaction (247–250 ppm, 5% O_2, Ar as balance).

Catalysts	CZ	Rh_{Cl}/CZ	Rh_N/CZ
T_{max} N_2 (°C)	325	260	360
Conversion of NO_x to N_2 (%)	28	6	52
HC conversion (%)	46	70	92
Total HC light-off temperature (°C)	350	250	240

presence of chloride ions on catalyst surface inhibiting the active sites. Such ions can only be removed by treatment at high temperature [35]. Hence, the chlorine contained in the sample Rh/$Ce_{0.62}Zr_{0.38}O_2$ after reduction at 500 °C is still 1.6 wt%, as determined by SEM–EDS.

Finally, Fig. 8 shows the evolution of NO_2 concentration in the course of NO oxidation (curve 1) and during TPSR (curve 2) in reaction mixture on Rh_N/CZ catalyst. One can see that in the temperature range in which deNO_x is observed (215–400 °C), NO_2 is almost eliminated in the presence of HC. This result suggests that NO_2 is strongly involved in the deNO_x process. We could suggest that NO_2 formation was lower in the presence of HC, because of competition for surface sites. However, in a previous study we already suggested that intermediates such as NO_2, RNO_x and oxygenates species from HC might be involved in the lean deNO_x process on CZ catalysts [12,14,36].

3.2.4. DeNO_x mechanism of ceria–zirconia-supported rhodium catalysts

The results of the present work show that the incorporation of Rh in nitrate form to CZ promotes significantly lean deNO_x activity.

3.2.4.1. Where does NO oxidation takes place?. It is now well known that during the deNO_x process, NO oxidation and NO dissociation

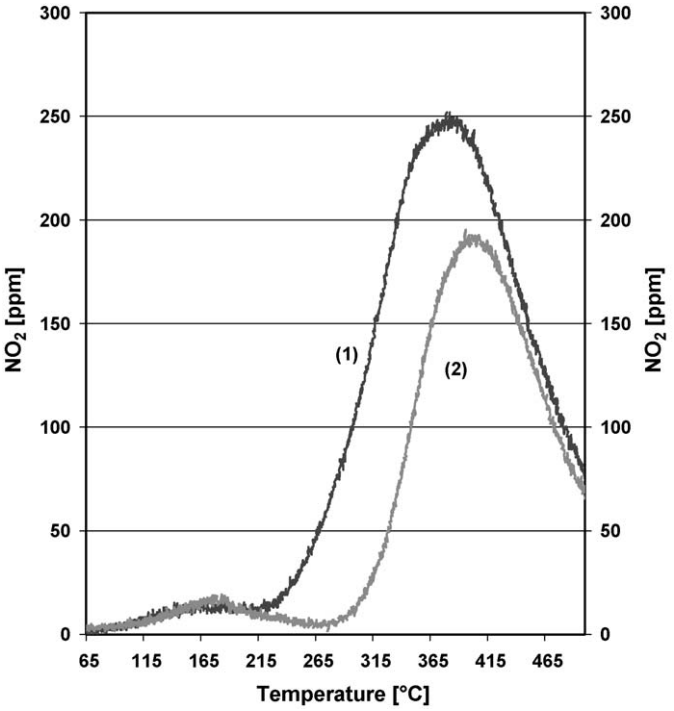

Fig. 8. Evolution of NO_2 concentration, ((1) black line) in the course of TPSR NO oxidation in presence of 250 ppm NO, 5% O_2, GHSV = 30,000 h^{-1}; ((2) grey line) in the course of TPSR in the presence of 247 ppm hydrocarbon mixture (propane, propene and toluene), 250 ppm NO, 5% O_2, GHSV = 30,000 h^{-1}; on Rh/$Ce_{0.625}Zr_{0.375}O_2$ (nitrate precursor).

are essential steps [12,14,15]. We first verified that NO_2 could be formed in the course of the deNO_x reaction. Thus, the NO oxidation was studied on the different supports.

As shown elsewhere [19] and confirmed in flue gases from coal combustion, the NO oxidation reaction was observed over bare CZ under TPSR conditions. The NO oxidation begins around 230 °C, is maximum around 420 °C then decreases. Furthermore, at high temperatures, the NO oxidation is limited by thermodynamics [12]. This reaction is thus catalyzed by the CZ support alone. These results are in agreement with the literature [12,18,19]. Thus, the NO oxidation can take place on sites from the support such as Ce^{3+}. However, the introduction of only Rh in nitrate form promotes the oxidation reaction. Thus, the effect of rhodium is different than those of palladium [12]. Finally, sites from the support or from Rh_2O_3 particles detected only in Rh_N samples are responsible of the NO oxidation.

3.2.4.2. NO_2–HC interaction. We already suggested that reaction intermediates such as NO_2, organic nitrogen-containing compounds (RNO_x) and oxygenates ($C_xH_yO_z$) might be involved in the lean deNO_x catalysis on CZ [18,19,36]. In the proposed mechanism, the production of NO_2 and $C_xH_yO_z$, the formation of the latter resulting from the decomposition of R-NO_x intermediates produced by the reaction of NO_2 and hydrocarbons such as C_3H_6, has been assumed to be critical for lean deNO_x activity, as also reported by other authors [37]. More recently, on chlorated ceria–zirconia-supported palladium catalysts, Thomas et al. [12,14] proposed a deNO_x mechanism based on three catalytic cycles, using propene as reductant. In this mechanism, the support achieves NO oxidation to NO_2, and NO decomposition to N_2, whereas PdO_x activates propene via ad-NO_x species, producing RNO_x compounds that subsequently decompose to NO and $C_xH_yO_z$. The role of these $C_xH_yO_z$ oxygenates is to reduce CZ to provide the catalytic sites responsible for NO decomposition. The RNO_x species have been identified for SCR of NO_x by hydrocarbons in excess of oxygen [18,36,38].

We have already shown that NO oxidation to NO_2 can be achieved on the support [19]. As already proposed on chlorinated CZ, the NO oxidation is then also possible on non-chlorinated CZ. On bare CZ, comparing deNO_x TPSR and NO oxidation TPSR, we can conclude that the activation of HC proceeds unambiguously also on support. Indeed, we have observed that the NO_2 production is lower during the TPSR under reaction mixture than during NO oxidation. As shown elsewhere [20], the nitrite anions are mainly formed during NO adsorption. The nitrites are transformed to nitrates as temperature increases. We can suppose that the nitrites formed interact with the hydrocarbons during the deNO_x process.

Moreover, during TPSR experiments, the concomitant HC activation and NO_x consumption lead to a large peak of CO_2. This large amount of CO_2 cannot be explained by HC total oxidation. However, it could be due to the formation of highly reactive oxygenate species ($C_xH_yO_z$) during the deNO_x process that further react with oxygen species (O_{ads}) strongly adsorbed on actives sites as proposed in the literature [16]. These $C_xH_yO_z$ could be alcohol or aldehyde species reported recently on alumina-supported Co–Pd catalyst for SCR NO_x by methane [39]. On bare CZ one could conclude that the NO_2 is also lower than expected and that again a large amount of CO_2 is observed in the range of deNO_x temperature. Thus, non-chlorinated CZ also activates the HC, leading to the same oxygenate species than for supported metals [12,15,16,18,19].

In presence of rhodium, coming from Rh_N samples, this activation is much higher; leading to the conclusion that rhodium oxide is an important site for the NO_2–HC reaction.

Indeed, from reaction mixture TPSR and in comparison with NO oxidation TPSR (Fig. 8), we can conclude that the activation of HC

proceeds unambiguously on the Rh_2O_3 catalytic function, as demonstrated by the hydrocarbons light-off temperature that decreases significantly over supported Rh catalysts (Table 4, Fig. 6). In addition, it is obvious that this low temperature activation of HC mixture is responsible for the lean deNO_x activity of Rh_N/CZ-based catalysts, as both HC mixture activation and deNO_x occur concomitantly (Figs. 4–6). Thus, the support might also activate the HC, leading to the same oxygenate species. Finally, these observations strongly suggest that NO_2 species adsorbed on the ceria–zirconia or Rh_2O_3 account for the activation of HC.

Several groups [31,32,40] have proposed that NO reduction takes place via a lacunar mechanism on reduced CZ sites. These authors, indeed, provided evidence for the decomposition of NO to N_2 on prereduced CeO_2 surfaces. Thomas et al. [12,14] confirmed these results on ceria–zirconia-supported PGM catalysts. The authors claimed that the decomposition of NO proceeds on the support. From Figs. 6 and 8, it seems more likely, that the NO_x reduction observed at low temperature (100–300 °C) is achieved on CZ, since the same activity is observed on the bare CZ and on the Rh_N/CZ catalyst. However, at higher temperature, CZ could not be the one responsible to the NO decomposition. Hence, at high temperature (>350 °C), the Rh_N/CZ is at least twice more active than the support alone. Furthermore, at high temperatures (>400 °C), thermodynamics limits the reaction. Then, the quantity of NO_2 formed on CZ and on Rh_N/CZ should be the same. Moreover, the amount of HC that can be activated is only about 200 ppm on Rh_N/CZ, and 600 ppm on CZ in steady-state conditions (Fig. 7). From these observations, one can conclude that a part of sites responsible for the decomposition of NO would, thus, be rhodium sites (Rh^{3+}). These sites have been already proposed for decomposition pathway in three-way catalysis in which CO is used as reductant [33]. Finally, the proposed mechanism is consistent with previous studies [12,15–17] who reported that three catalytic functions were required for the occurrence of the SCR of NO_x by hydrocarbons. Moreover, as already suggested in the literature [12,14,19], CZ achieves both NO oxidation to NO_2 (cycle 1) and NO decomposition to N_2 (cycle 3), whereas Rh_2O_3 activates the hydrocarbons via ad-NO_2 species (cycle 2) intermediately producing R-NO_x compounds that further decompose to NO and $C_xH_yO_z$. The role of the latter oxygenates is to reduce CZ to provide the catalytic sites responsible for NO decomposition (cycle 3). However, Rh_N/CZ catalysts the rhodium species such as Rh_2O_3 achieve the NO oxidation whereas Rh^{3+} species or lacunar Rh_2O_3 species are the active species during NO dissociation which should lead to N_2: (i) the adsorption of two NO molecules, (ii) the dissociation of 2NO leaving oxygen species (O_{ads}) strongly adsorbed on actives sites, (iii) the necessity, for the reductant, to scavenge the $2O_{ads}$, for recovering the free sites and permitting the reaction to turn over [15]. The NO reduction for deNO_x process can mainly occur over M^{x+} catalytic sites going to the N_2 formation through N_2O intermediate. Depending on the nature of the cation and temperature, N_2O can desorb or transform to N_2 depending on the set of rate constants.

4. Conclusion

The TPSR and steady-state experiments carried out on ceria–zirconia and on Rh_N/CZ show that both support and Rh/CZ catalyst are active in coal deNO_x reaction. Furthermore, Rh_{Cl}/CZ catalyst shows lower NO_x conversions to N_2 than Rh_N/CZ catalyst and than bare support. It was supposed that chlorine ions present on catalyst surface inhibit the active sites and in consequence reduce the catalytic activity. The obtained results reveal that rhodium addition impregnated by nitrate precursor, considerably improves catalytic activity of CZ in the deNO_x process. A maximum of 52% conversion is observed at 360 °C. On Rh_N/CZ catalyst, Rh_2O_3 and Rh^{3+} phases have been observed by XPS and TEM analyses.

No metallic Rh species were detected by PME measurements on catalysts following treatment in oxidizing conditions.

On this catalyst, the three functions are involved in deNO_x proceed simultaneously: (i) oxidation of NO to NO_2 on support or on Rh_2O_3 particles, (ii) mild oxidation of HC in the presence of NO_2 to oxygenate $C_xH_yO_z$ on Rh_2O_3 and (iii) decomposition-reduction of NO to N_2 with total oxidation of oxygenated species, on support or on (Rh^{3+} species from Rh_2O_3).

The reproducibility of the catalyst was verified and clearly showed the same activity. Experiments in presence of water are in progress. Moreover, runs will be performed using a monolithic form of the catalyst in real coal deNO_x conditions in a lab-scale device then in a micro-pilot plant device.

Acknowledgements

The authors want to thank to Patricia Beaunier and Dr. Marie Dominique Appay for TEM study and analysis.

Appendix A. Supplementary data

Supplementary data associated with this article can be found, in the online version, at doi:10.1016/j.apcatb.2009.04.018.

References

[1] V.I. Pârvulescu, P. Grange, B. Delmon, Catal. Today 46 (1998) 233.
[2] R. Burch, J.P. Breen, F.C. Meunier, Appl. Catal. B: Environ. 39 (2002) 283.
[3] M. Wojciechowska, S. Lomnicki, Clean Prod. Process. 1 (1999) 237.
[4] K.A. Bethke, M.C. Kung, B. Yang, M. Shah, D. Alt, C. Li, H.H. Kung, Catal. Today 26 (1995) 169.
[5] Y. Nagai, T. Yamamoto, T. Tanaka, S. Yoshida, T. Nonaka, T. Okamoto, A. Suda, M. Sugiura, Catal. Today 74 (2002) 225.
[6] L.F. de Mello, M. Auxiliadora, S. Baldanza, F.B. Noronha, M. Schmal, Catal. Today 85 (2003) 3.
[7] R. Burch, D. Ottery, Appl. Catal. B: Environ. 13 (1997) 105.
[8] A.B. Ross, J.M. Jones, S. Chaiklangmuang, M. Pourkashanian, A. Williams, K. Kubica, J.T. Andersson, M. Kerst, P. Danihelka, K.D. Bartle, Fuel 81 (2002) 571.
[9] S.N. Orlik, V.L. Struzhko, T.V. Mironyuk, G.M. Tel'biz, Theor. Exp. Chem. 37 (2001) 311.
[10] G. Centi, P. Fornasiero, M. Graziani, J. Kašpar, F. Vazzana, Top. Catal. 16–17 (2001) 157.
[11] L.F. Liotta, A. Longo, A. Macaluso, A. Martorana, G. Pantaleo, A.M. Venezia, G. Deganello, Appl. Catal. B: Environ. 48 (2004) 133.
[12] C. Thomas, O. Gorce, C. Fontaine, J.-M. Krafft, F. Villain, G. Djéga-Mariadassou, Appl. Catal. B: Environ. 63 (2006) 201.
[13] R. Burch, P.J. Millington, A.P. Walker, Appl. Catal. B: Environ. 4 (1994) 65.
[14] C. Thomas, O. Gorce, F. Villain, G. Djéga-Mariadassou, J. Mol. Catal. A 249 (2006) 71.
[15] G. Djéga-Mariadassou, Catal. Today 90 (2004) 27.
[16] G. Djéga-Mariadassou, M. Boudart, J. Catal. 216 (2003) 320.
[17] A.P. Ferreira, S. Capela, P. Da Costa, C. Henriques, M.F. Ribeiro, F.R. Ribeiro, Catal. Today 119 (2007) 156.
[18] O. Gorce, F. Baudin, C. Thomas, P. Da Costa, G. Djéga-Mariadassou, Appl. Catal. B: Environ. 54 (2004) 69.
[19] M. Adamowska, S. Muller, P. Da Costa, A. Krztoń, P. Burg, Appl. Catal. B: Environ. 74 (2007) 278.
[20] M. Adamowska, A. Krztoń, M. Najbar, P. Da Costa, G. Djéga-Mariadassou, Catal. Today 137 (2008) 288.
[21] F. Fajardie, J.-F. Tempère, J.-M. Manoli, O. Touret, G. Blanchard, G. Djéga-Mariadassou, J. Catal. 179 (1998) 469.
[22] D.I. Kondarides, X.E. Verykios, J. Catal. 174 (1998) 52.
[23] S.H. Overbury, D.R. Mullins, in: A. Trovarelli (Ed.), Ceria Surfaces and Films for Model Catalytic Studies Using Surface Analysis Techniques, Imperial College Press, London, 2002, p. 328.
[24] F. Fajardie, J.-F. Tempère, G. Djéga-Mariadassou, G. Blanchard, J. Catal. 163 (1996) 77.
[25] M. Zimowska, J.B. Wagner, J. Dziedzic, J. Camra, B. Borzecka-Prokop, M. Najbar, Chem. Phys. Lett. 417 (2006) 137.
[26] D. Terribile, A. Trovarelli, J. Llorca, C. de Leitenburg, G. Dolcetti, Catal. Today 43 (1998) 79.
[27] Z.W. Sieh, R. Gronsky, A.T. Bell, J. Catal. 170 (1997) 62.
[28] S. Suhonen, M. Valden, M. Hietikko, R. Laitinen, A. Savimaki, M. Harkonen, Appl. Catal. A: Gen. 218 (2001) 151.

[29] A.D. Logan, A.K. Datye, J.E. Houston, Surf. Sci. 245 (1991) 280.
[30] P. Burtin, J.P. Brunelle, M. Pijolat, M. Soustelle, Appl. Catal. 34 (1987) 239.
[31] M. Daturi, N. Bion, J. Saussey, J.-C. Lavalley, C. Hedouin, T. Seguelon, G. Blanchard, Phys. Chem. Chem. Phys. 3 (2001) 252.
[32] A. Martinez-Arias, J. Soria, J.C. Conesa, X.L. Soane, A. Arcoya, R. Cataluna, J. Chem. Soc., Faraday Trans. 91 (1995) 1679.
[33] G. Djéga-Mariadassou, F. Fajardie, J.-F. Tempère, J.-M. Manoli, O. Touret, G. Blanchard, J. Mol. Catal. A: Chem. 161 (2000) 179.
[34] C. Force, J.P. Belzunegui, J. Sanz, A. Martínez-Arias, J. Soria, J. Catal. 197 (2001) 192.
[35] K. Eguchi, S. Kikuyama, Catal. Surv. Jpn. 6 (2002) 55.
[36] F. Baudin, P. Da Costa, C. Thomas, S. Calvo, Y. Lendresse, S. Schneider, F. Delacroix, G. Plassat, G. Djéga-Mariadassou, Top. Catal. 30–31 (2004) 97.
[37] K.O. Haj, S. Ziyade, M. Ziyad, F. Garin, Appl. Catal. B: Environ. 37 (2002) 49.
[38] V.A. Sadykov, V.V. Lunin, V.A. Matyshak, E.A. Paukshtis, A.Y. Rozovskii, N.N. Bulgakov, J.R.H. Ross, Kinet. Catal. 44 (2003) 379.
[39] R. Marques, K. El Kabouss, P. Da Costa, S. Da Costa, F. Delacroix, G. Djéga-Mariadassou, Catal. Today 119 (2007) 166.
[40] S.H. Overbury, D.R. Mullins, D.R. Huntley, L.J. Kundakovic, J. Catal. 186 (1999) 296.